Received: 27 August 2018 | Revised: 14 June 2019 | Accepted: 15 July 2019

DOI: 10.1002/joc.6232

RESEARCH ARTICLE

International Journal of Climatology RMetS

Role of autumn Arctic Sea ice in the subsequent summer precipitation variability over East Asia

Yang Liu[1,2,3] | Yali Zhu[1,2,4] | Huijun Wang[1,2,4] | Yongqi Gao[1,5] | Jianqi Sun[1,2,4] | Tao Wang[1,2,4] | Jiehua Ma[1,2,4] | Alla Yurova[6,7] | Fei Li[8]

[1]Chinese Academy of Sciences, Institute of Atmospheric Physics, Nansen-Zhu International Research Center, Beijing, People's Republic of China

[2]Chinese Academy of Sciences, Climate Change Research Center, Beijing, People's Republic of China

[3]University of Chinese Academy of Sciences, Beijing, People's Republic of China

[4]Nanjing University for Information Science and Technology, Key Laboratory of Meteorological Disaster/Collaborative Innovation Center on Forecast and Evaluation of Meteorological Disasters, Nanjing, Jiangsu, People's Republic of China

[5]Bjerknes Centre Climate Research, Nansen Environment and Remote Sensing Centre, Bergen, Norway

[6]Institute of the Earth Science, Saint Petersburg State University, Universitetskaya nab, St. Petersburg, Russia

[7]Scientific Foundation "Nansen International Environmental and Remote Sensing Centre", St. Petersburg, Russia

[8]NILU-Norwegian Institute for Air Research, Kjeller, Norway

Correspondence
Yali Zhu, Nansen-Zhu International Research Center, Institute of Atmospheric Physics Chinese Academy of Sciences, Huayanli 40 Street, Chaoyang District, Beijing 100029, China.
Email: zhuyl@mail.iap.ac.cn

Funding information
National Key Research and Development Program of China, Grant/Award Number: 2016YFA0600701; National Natural Science Foundation of China, Grant/Award Numbers: 41611130043, 41675083, 41605064; CAS-PKU Joint Research Program

Abstract

This study explored the interannual relationship between autumn Arctic sea ice concentration (SIC) and the subsequent summer precipitation over East Asia (EASP). Since the late-1990s, the declining SIC in the Kara–Laptev Seas has been significantly correlated with EASP as well as extremely positive anomalies in northern China and intensely negative anomalies in central-eastern East Asia. However, there was a weak correlation between autumn SIC and EASP before the late-1990s. Furthermore, the anomalous precipitation pattern in summer and its connection with autumn SIC variability can be explained by the seasonal persistence of continental processes (snow depth and soil moisture) into the spring. In particular, a decreasing SIC was connected with simultaneously positive and negative precipitation anomalies over northeastern China and the Siberian region, respectively, since the late-1990s and tends to produce corresponding soil moisture anomalies over the Eurasian continent. Declining SIC also favours increased snow depth anomalies in winter over northeastern East Asia. These anomalous signals of surface processes can persist from winter into the subsequent spring, making the connection between the autumn SIC and EASP possible. The Community Earth System Model Large Ensemble simulations further verified these physical processes. More detailed mechanism for this relationship needs to be stressed in further work by numerical simulations. The results have important implications for extending the seasonal prediction validity of EASP. Moreover, before the late-1990s, SIC-related circulation anomalies shifted westward and northward as negative precipitation anomalies developed over west Siberia in autumn. As a result, anomalous dry soil conditions in Siberia persisted into the subsequent spring and then led to wetter-than-normal conditions through locally negative soil moisture–precipitation feedback before the late-1990s.

KEYWORDS
Arctic Sea ice, precipitation over East Asia, seasonal prediction, snow depth, soil moisture

1 | INTRODUCTION

East Asian summer (June–August) precipitation (EASP) contributes most of the annual precipitation over East Asia and its interannual variability usually shows a tripole anomaly pattern (Hsu and Liu, 2003; Hsu and Lin, 2007; Wang and He, 2015), with one centre over central-eastern China and Japan and two opposite centres over northern and southern China (Hsu and Lin, 2007; Wang and He, 2015). Previous studies have suggested that the EASP anomaly is related to the evolution of El Nino-Southern Oscillation (ENSO; Weng *et al*., 1999; Ding and Wang, 2005; Yim *et al*., 2014; Fu and Lu, 2017). Xie *et al*. (2009) focused on interannual variability and showed that the increased SSTs over the tropical Indian Ocean (TIO) induced the Pacific-Japan (PJ) pattern via simulating the equatorial Kelvin wave, which led to a suppression of deep convection in the northwestern Pacific. In addition, the PJ pattern, related to active convection over the tropical western Pacific, is a dynamical mode and can draw energy from the summer mean flow and EASP (Nitta, 1987; Kosaka and Nakamura, 2006). Another wave train, the Silk Road pattern, is related to interannual variability of the tripole precipitation pattern by emitting anomalous signals across the Eurasian continent (Hsu and Lin, 2007). Furthermore, recent studies have implicated the impact of other forces on the occurrence of precipitation anomalies. For example, diabatic heating over the Tibetan Plateau affects summer precipitation interannual variability by triggering a Rossby wave (Hsu and Liu, 2003). This precipitation anomaly is tied to the meridional migration of the westerly winds relative to the Plateau region (Hsu and Lin, 2007; Chiang *et al*., 2017). These past studies mostly concentrated on the linkage between precipitation anomaly patterns and mid- and lower-latitudes circulations.

However, climate systems in high latitudes can also exert widespread, significant impacts on worldwide climate. The rapid decline in Arctic sea ice since 1979 has received much attention in the past decades. This decline has had pronounced impacts on global atmospheric circulation via the resulting increase in absorption of solar energy by the change in surface albedo, called the ice-albedo feedback mechanism (Curry *et al*., 1995). The influence of autumn Arctic sea ice loss on Northern Hemisphere winter climate has drawn considerable attention in recent studies (McBean *et al*., 2005; Budikova, 2009; Bader *et al*., 2011; Vihma, 2014; Gao *et al*., 2015). In addition, winter sea ice anomalies west of Greenland have a significant correlation with the anomalous atmospheric circulation wave train, and affect northern European precipitation variability in the following summer (Wu *et al*., 2013). Screen (2013) used modelling experiments forced by seasonal sea ice to suggest that reducing Arctic sea ice (over the entire region) may contribute to incremental summer precipitation in Europe.

There have also been studies that investigated the impact of spring Arctic sea ice on summer precipitation over Eurasia. A number of studies have also addressed the impact of high-latitude forcing on EASP (Zhao *et al*., 2004; Wu *et al*., 2013). Zhao *et al*. (2004) pointed out that stationary wave activity and land surface processes may explain the influence of the anomalous decrease in spring sea ice on the enhancement of summer precipitation over East Asia. However, Guo *et al*. (2014) noted that this close relationship could be explained by the persistence of anomalous SST in the North Pacific.

Previous studies mainly investigate the role of recent autumn Arctic sea ice loss on the boreal winter climate (Li and Wang, 2012; Liu *et al*., 2012; Gao *et al*., 2015). Arctic sea ice declines more rapidly in the autumn than in the other seasons, and the links between autumn Arctic sea ice and the following summer climate have received far less scientific attention. A better understanding of this topic will help us to identify potential precursor of summertime precipitation variability over East Asia. In fact, due to sea-ice loss, more heat stored in the Arctic Ocean is released into the air, and then affects the circulation locally and remotely (Screen and Simmonds, 2010; Kim *et al*., 2014). Accordingly, anomalous circulations have impacts on the land physical properties (e.g., snow and soil). Snow and soil, as the slowly varying components of the system, are likely to be media to link following circulations due to the long time scale over their variations (Entin *et al*., 2000; Koster *et al*., 2014, 2016). Focusing on boreal summer, Koster *et al*. (2016) demonstrated the impact of anomalous soil moisture on the local and remote atmosphere with a series of stationary wave model simulations. For local impact, wet soil can decrease the surface temperature via increasing evapotranspiration, which in turn leads to cooling the surface air; it can also alter the boundary-layer stability, which perhaps leads to precipitation formations (Hohenegger *et al*., 2009; Seneviratne *et al*., 2010). As for non-local impact, soil moisture anomalies may lead to remotely atmospheric circulation variations through Rossby waves (Douville, 2002; Koster *et al*., 2014) or atmospheric patterns (Lau and Kim, 2012). Moreover, several studies have also investigated the role of snow cover on atmospheric general circulation (Peings *et al*., 2013; Cohen *et al*., 2014). The aim of the present study is to extend previous studies on the potential relationship between the autumn Arctic sea ice concentration (SIC) and the subsequent anomalous summer precipitation pattern over East Asia during the past three decades at an interannual timescale, and finally provide valuable information for the seasonal prediction of East Asian summer rainfall.

2 | DATA AND METHODS

2.1 | Observational datasets

A new version of SICs on a 1° latitude-longitude grid from 1850 to present is retrieved from the Met Office Hadley Centre, HadISST.2.2.0.0 (Titchner and Rayner, 2014). It is worth noting that HadISST.2.2.0.0 contains more ice and higher concentrations than the previous version (Titchner and Rayner, 2014). The monthly precipitation dataset, based on a combination of satellite and observational data, is derived from the Global Precipitation Climatology Project (GPCP) for the period from 1979 to present, at a horizontal resolution of 2.5° × 2.5° (Adler *et al*., 2003). Monthly atmospheric reanalysis products at a resolution of 2.5° were obtained from the National Centers for Environmental Prediction–Department of Energy (NCEP-DOE; Kanamitsu *et al*., 2002). Monthly soil moisture data, covering the period from 1979 to 2016, are obtained from the European Centre for Medium Range Weather Forecast's Interim reanalysis (ERA-Interim) dataset (Dee *et al*., 2011). The ERA-Interim data are from depths of 0–7, 7–28, 28–72 and 72–189 cm below the surface, at a resolution of 0.5° × 0.5°. Here we used the soil moisture in the top two layers (0–7 and 7–28 cm), given that the soil moisture in the subsurface layer is more active than in the deep layer (Yang *et al*., 2016). Additionally, another monthly dataset of soil moisture, obtained from the Climate Prediction Center (CPC) of National Oceanic and Atmospheric Administration (Fan and van den Dool, 2004; https://www.esrl.noaa.gov/psd/data/gridded/data.cpcsoil.html), was introduced to reduce the uncertainty of the ERA-Interim soil moisture dataset. The CPC soil moisture, calculated by a one-layer hydrological model, has no vertical profile (Van den Dool *et al*., 2003). The 1° × 1° resolution daily snow depth dataset was obtained from an unofficial release of ERA-Interim for the period from January 1981 to December 2014 (Wegmann *et al*., 2017). We also made use of soil moisture and snow depth data provided by Modern-Era Retrospective analysis for Research and Application, Version 2 (MERRA-2). MERRA-2 is a global atmospheric reanalysis that assimilates both conventional and satellite observations and begins in 1980, at an approximate resolution of 0.5° × 0.625° (Bosilovich *et al*., 2015).

Monthly mean Nino-3.4 index, an ENSO indicator, is defined as the average SST anomalies in the domain (5°S–5°N, 170°W–120°W; Rayner *et al*., 2003; the data used herein were obtained online at https://www.esrl.noaa.gov/psd/gcos_wgsp/Timeseries/Nino34/for1870-present).

2.2 | Modelling datasets

The Community Earth System Model Large Ensemble (CESM-LE) simulations (Kay *et al*., 2015), performed by the Community Earth System Model version 1 with the Community Atmosphere Model version 5 (CESM1-CAM5), are used to provide additional evidence in this study. CESM1-CAM5, coupled with atmosphere, ocean, land and sea ice at approximately 1° latitude-longitude, is a fully coupled climate model (Hurrell *et al*., 2013). Forty ensembles are included in CESM-LE covering the period 1920–2100 (historical forcing up to 2005 and Representative Concentration Pathway 8.5 [RCP8.5] forcing from 2006 to 2100). A detailed description of the CESM-LE is provided in Kay *et al*. (2015). Here, we mainly use monthly datasets from CESM-LE.

2.3 | Methods

The months of September–November (SON), December–February (DJF), March–May (MAM) and June–August (JJA) are used to represent autumn, winter, spring and summer seasons, respectively. Anomalies were calculated by subtracting the climatology. To reveal the dominant modes of covariability between the Arctic autumn SIC and summer precipitation, we used the singular value decomposition (SVD) method. SVD is a fundamental matrix operation and a generalization of a diagonalization procedure that is performed in the principal component analysis to matrices that are not square or symmetric (Bretherton *et al*., 1992). This analysis is performed on the covariance matrix using weights proportional to the area of the grid between the two space data fields.

Regression and correlation analyses are carried out to calculate the precipitation and atmospheric circulation anomalies that are present during summer and are associated with the sea ice indices from the previous autumn and the significance of the results is assessed with the two-tailed Student's *t* test. To eliminate the possible linear influence of ENSO while exploring the possible mechanism for how autumn Arctic sea ice affects the ensuing summer precipitation pattern over East Asia, we applied a linear regression to the variable, with regard to the simultaneous Nino-3.4 index, and then calculated the residual, which was the difference between the raw variable and the regressed variable. The linear trend is removed for the whole analysis period from all aforementioned data before analysis.

3 | COVARIABILITY BETWEEN AUTUMN ARCTIC SEA ICE AND THE ENSUING SUMMER PRECIPITATION PATTERN OVER EAST ASIA

The SVD technique is used to examine the covariability between the autumn Arctic SIC and EASP for the last three decades. Figure 1 illustrates the spatial pattern of the first

SVD mode of Arctic SIC in the Kara–Laptev Seas and precipitation anomalies over East Asia, which accounts for approximately 51% of the total covariance. The temporal expansion coefficients are highly correlated, with a value of 0.68 (Figure 1c), which is significant at the 99% confidence level. When the autumn Arctic SIC in the Kara–Laptev Seas is below normal (Figure 1a), the northern part of East Asia experiences considerably higher-than-normal precipitation along with lower-than-normal over central-eastern China, South Korea and south of Japan (Figure 1b). This precipitation anomaly distribution closely resembles the tripole precipitation pattern reported by Hsu and Lin (2007), which is characterized by one centre over central-eastern China and Japan, and two opposite centres over northern and southern China. Since the anomalous centre over southern East Asia is not clear in our study, we only discuss the northern and central centres of the tripole structure. Additionally, the EASP variation in the leading SVD (Figure 1b) highly resembles the leading empirical orthogonal function (EOF) of precipitation anomalies over East Asia (figure not shown), indicating a dominant pattern of EASP variability.

The SIC index is denoted by the time series of leading SVD for autumn SIC (multiplied by −1, corresponding to a negative unit departure of SVD1-SIC). Since this index is closely correlated with the area-weighted mean SIC anomalies over the Kara–Laptev Seas (70°−85°N, 60°−130°E; with a coefficient of −0.98, at a 99% significance level), it could represent sea ice variations in the Kara–Laptev Seas. Negative values indicate below normal SIC in the Kara–Laptev Seas, as shown in Figure 2a. Correspondingly, the time series of the leading SVD for EASP is regarded to be the precipitation index (PI). Figure 2b displays the regression of precipitation anomalies with regard to the PI. It suggests that the PI could represent the precipitation anomaly pattern over East Asia, as well as the positive and negative anomalies over the northern part of East Asia and southern Japan, respectively, which highly resembles the spatial pattern of the leading SVD for EASP (Figure 1b). Moreover, corresponding temporal expansion coefficients display more same-sign values after the late-1990s, suggesting a potential interdecadal shift in their relationship (Figure 1c). Figure 2c verifies this unstable relationship by presenting 19-year sliding correlation coefficients for these two time series, and the correlation between SIC and EASP is significant at the 95% confidence level after the late-1990s. In contrast, the correlation is not significant before the late-1990s. Thus, a weak and a robust correlation period was selected before and after the late-1990s, respectively, to study the unstable correlation between SIC and EASP. The central years of the 19-year window are approximately the years 1987/1988 and 2004/2005, when the correlation is the lowest and highest, respectively. This means that the SIC-EASP relationship seems insignificantly correlated during 1979/1980–1995/1996 (simplified as 1980–1996, with a coefficient of 0.23), but significantly correlated during 1996/1997–2015/2016 (simplified as 1997–2016, with a coefficient of 0.85).

Therefore, we show the distribution of precipitation and circulation conditions during 1980–1996 and 1997–2016, respectively, to understand the relationship between autumn Arctic sea ice and EASP during the past three decades. Figure 3 shows the summer precipitation anomalies, relevant atmospheric circulation and upper troposphere divergence anomalies regressed onto the SIC index during the two sub-

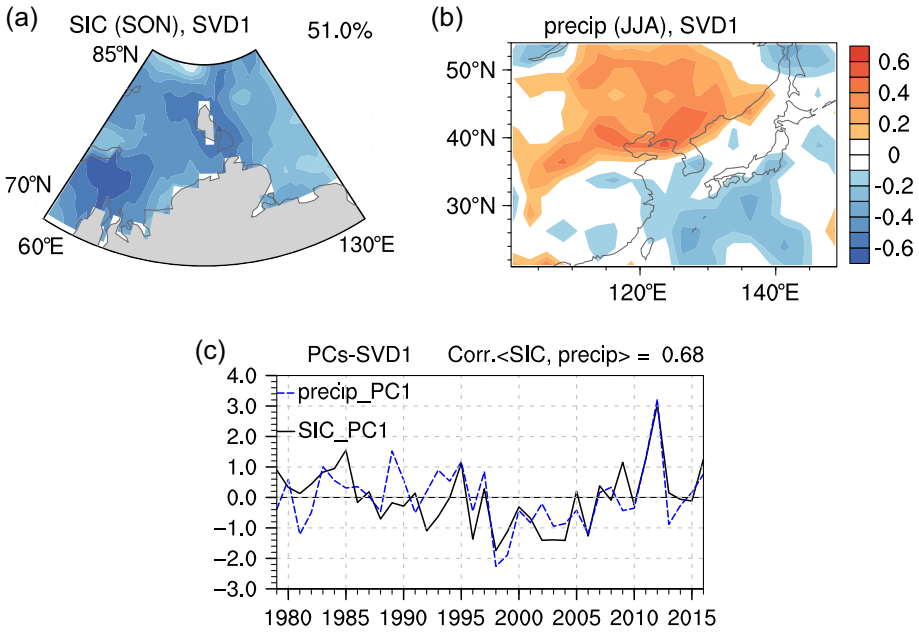

FIGURE 1 First SVD mode of autumn SIC and subsequent summer precipitation for the period 1979/1980–2016/2017. (a) The spatial pattern of SVD1-SIC; (b) the spatial pattern of SVD1-precipitation; (c) the corresponding time series

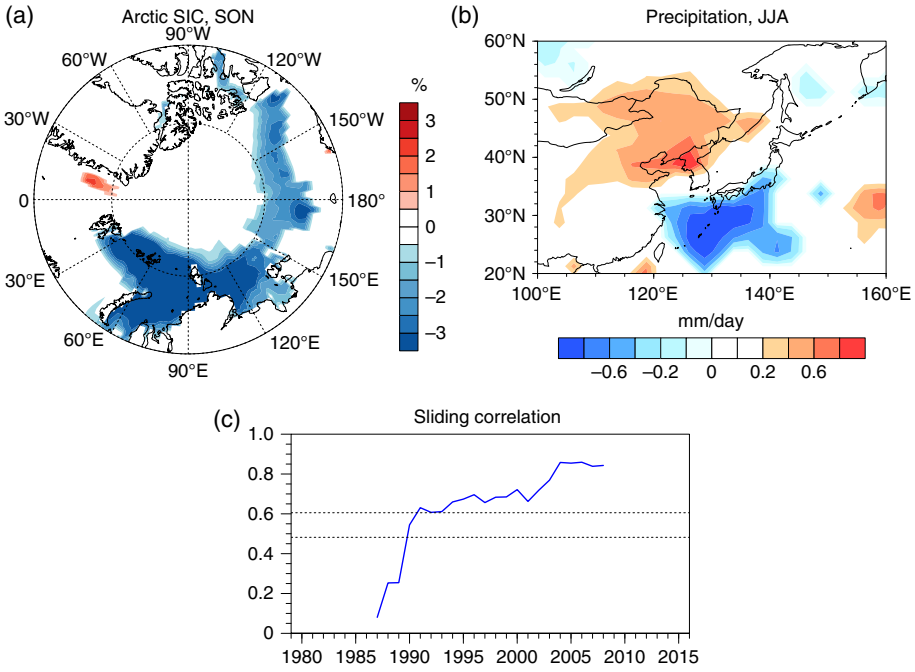

FIGURE 2 Regression maps of (a) autumn SIC anomalies with regard to SIC index and (b) summer precipitation anomalies (mm/day) with regard to PI during 1979/1980–2016/2017. Only significant values at the 90% confidence level from a two-tailed Student's *t* test are shaded. (c) 19-Year sliding correlation coefficients between SVD1-SIC and SVD1-PI. The dashed lines denote a significance level of 95 and 99%, respectively

periods. Notable differences appear in the autumn SIC-related precipitation anomalies between the two periods (Figure 3a,d). During the period 1980–1996, associated with the sea ice loss, precipitation anomalies are not significant over East Asia. However, positive and significant precipitation anomalies are observed east of the Ural, and negative anomalies are seen east of the Baikal (Figure 3a). In contrast, during the period 1997–2016, the spatial distribution of anomalous precipitation in summer exhibits a dipole structure over East Asia, characterized by a positive and a negative precipitation anomaly centre over northern and central-eastern East Asia, respectively (Figure 3d). This anomalous pattern resembles the first leading SVD of EASP (Figure 1b), suggesting a close connection between SIC and EASP mainly occurs after the late-1990s. Correspondingly, the conditions in atmospheric circulation during 1980–1996 and 1997–2016 are also displayed in Figure 3. During the period 1997–2016, an anomalous surface cyclonic circulation is obvious in central Eurasia (35°−55°N, 100°−130°E), along with negative sea level pressure (SLP) anomalies, suggesting stronger-than-normal southwesterlies over northeastern East Asia (Figure 3e). In addition, there is an anomalous surface anticyclonic circulation south of Japan, along with positive SLP anomalies, indicating anomalous northeasterlies over the East China Sea (Figure 3e). Divergence in the 200 hPa winds appears over northern East Asia alongside low-level convergence, which tends to cause moisture to converge and then leads to anomalous ascending motion (Figure 3f). However, the conditions south of Japan are unfavourable for moisture condensation and then leads to the descending anomalies linked to upper-level convergence and lower-level divergence (Figure 3f). As a result, the air humidity over northern East Asia (south of Japan) increases (decreases) significantly, leading to a dipole pattern of anomalous wet conditions over northern East Asia and dry conditions south of Japan (Figure 3d). Therefore, these results validate the significant relationship between autumn Arctic sea ice anomalies and summer precipitation patterns in East Asia from 1997–2016. During 1980–1996, on the contrary, significant circulation anomalies are not seen over East Asia, implying that the autumn sea ice does not exert a marked impact on the following EASP during this period. Meanwhile, a pronounced low-level cyclonic circulation anomaly appears over west Siberia, along with a negative sea level pressure (SLP) anomaly (Figure 3b). High-level divergence winds in this region are favoured to gather moisture due to upward motion (Figure 3c), leading to wet conditions over west Siberia (Figure 3a). The notable differences in the autumn sea ice-related precipitation and the atmospheric circulation anomalies over East Asia between the two sub-periods suggest an enhanced connection of SIC-EASP in the subsequent summer, beginning after the late-1990s.

4 | POSSIBLE LINKAGE MECHANISMS AND MODELLING EVIDENCE

How does the changing autumn Arctic sea ice exert disparate impacts on the ensuing summer precipitation anomalies over Eurasian continents? When sea ice melts, the albedo is reduced and a large amount of solar heat enters and warms the upper ocean. During freezing, open-water exerts an influence on subsequent seasons' atmospheric circulation via

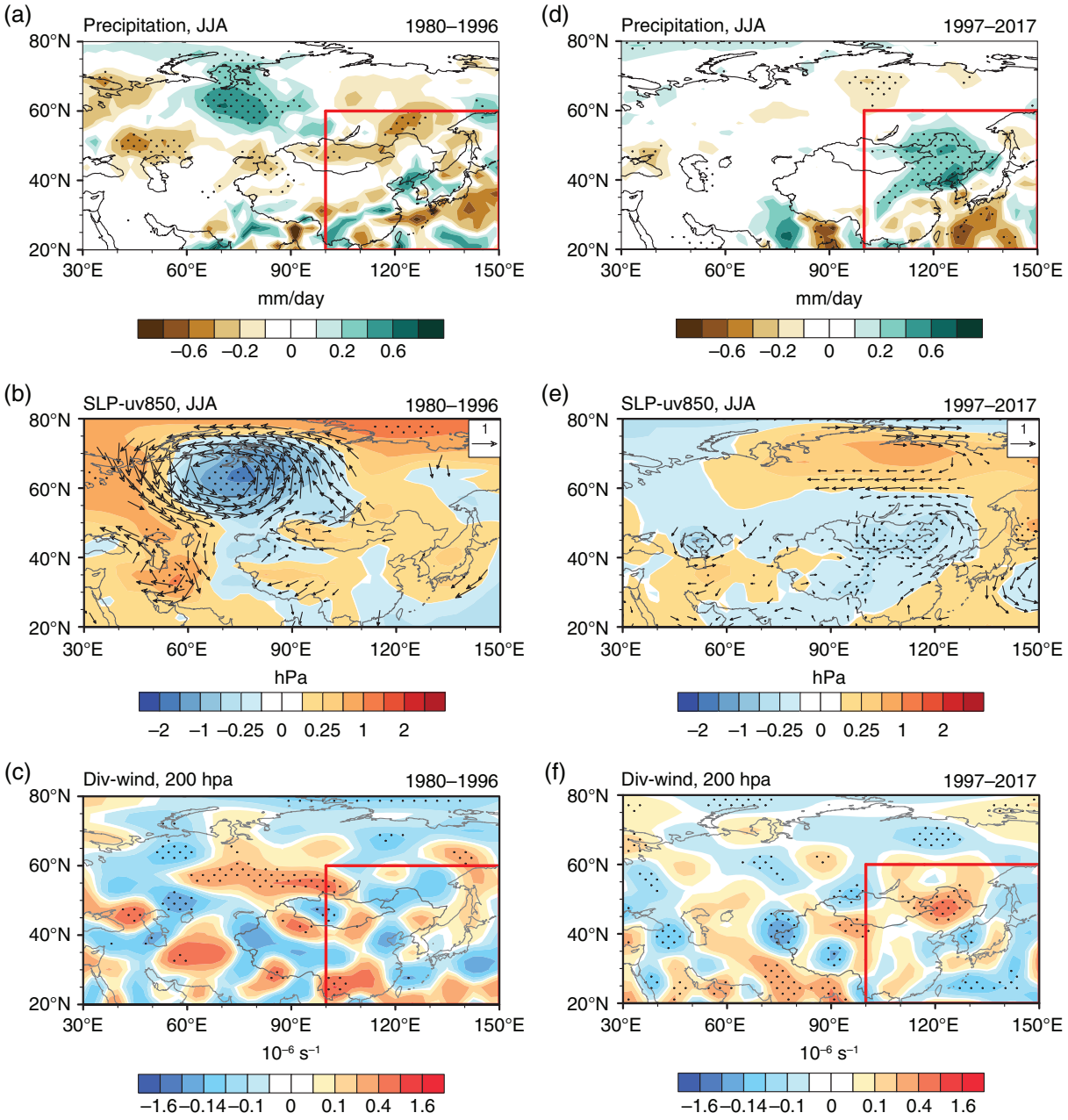

FIGURE 3 Regression maps of (a) summer precipitation anomalies (mm/day), (b) SLP (shading; hPa) and 850 hPa winds (vectors; m/s), and (c) divergence at 200 hPa (10^{-6} s^{-1}) with regard to SIC during 1979/1980–1995/1996. The right panel (d–f) is the same as the left panel (a–c), but from 1996/1997–2016/2017. Vectors and stippled regions denote the values significant at the 90% confidence level from a two-tailed Student's *t* test

surface heat and moisture flux (Liu *et al*., 2012). As mentioned previously, an increasing number of studies have revealed that reduced autumn Arctic sea ice has an impact on the Eurasian climate in subsequent seasons (Deser *et al*., 2010; Francis and Vavrus, 2012; Liu *et al*., 2012; Zuo *et al*., 2016). That is, following anomalous sea ice loss in autumn, the fluctuations in boreal winter circulation resemble the negative phase of the Arctic Oscillation (Liu *et al*., 2012; Mori *et al*., 2014), and include increased snowfall in the Northern Hemisphere (Liu *et al*., 2012). To understand what causes the interdecadal change in the autumn sea ice-summer precipitation relationship, we first detect the simultaneous autumn atmospheric circulation and precipitation anomalies regressed upon the SIC index during the periods 1980–1996 and 1997–2016. Figure 4 displays the anomalous high- and low-level atmospheric circulation, as well as precipitation anomalies, related to the SIC index during the two sub-periods. During the period of 1980–1996, when sea ice anomalies were below normal, high-level geopotential height anomalies illustrate a meridional seesaw pattern

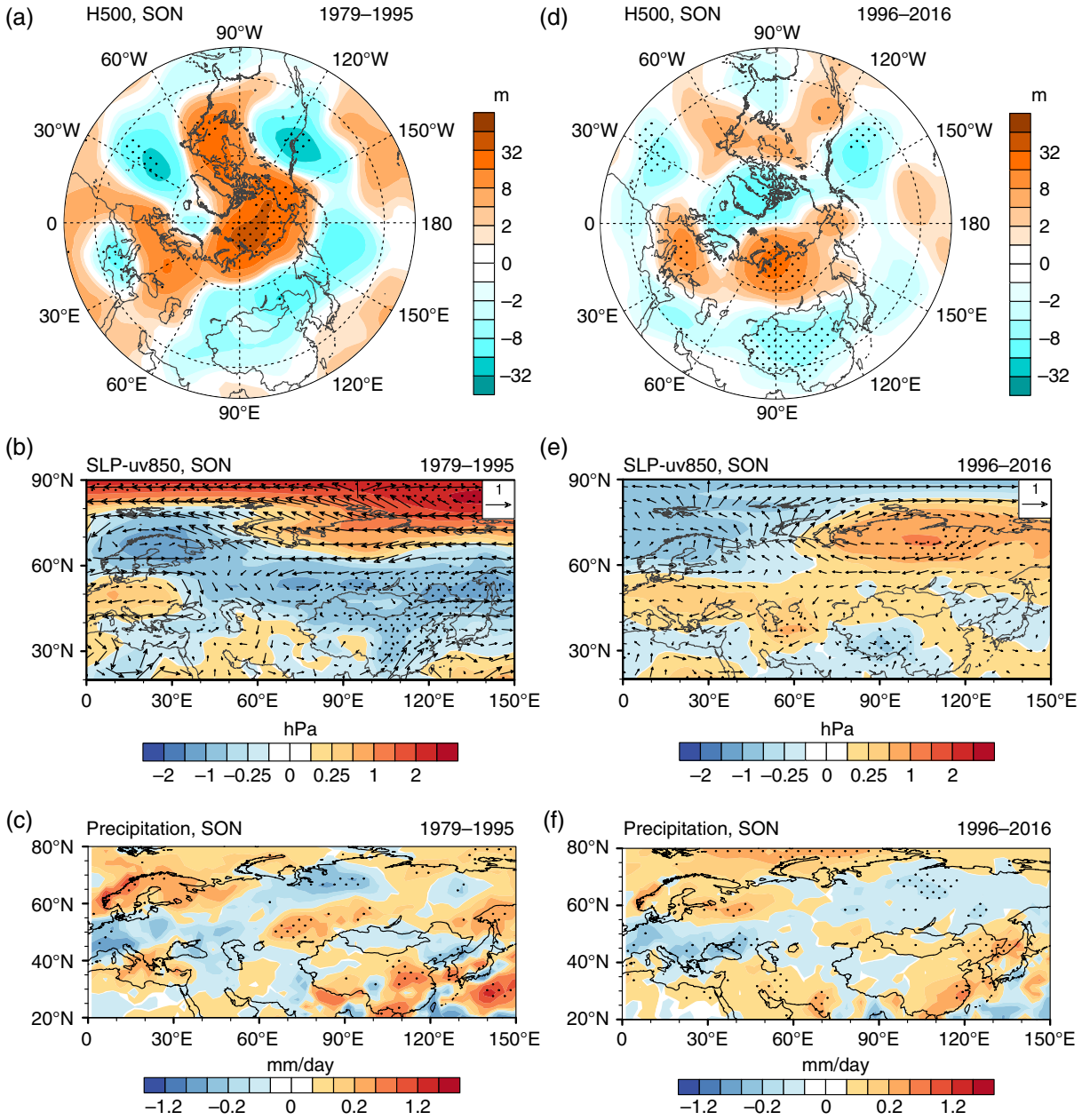

FIGURE 4 Regression maps of autumn (a) geopotential height anomalies at 500 hPa (m), (b) SLP (shading; hPa) and 850 hPa winds anomalies (vectors; m/s), and (c) precipitation anomalies (mm/day) with regard to autumn SIC index during 1979–1995. The right panel (d–f) is the same as the left panel (a–c), but from 1996–2016. Stippled regions denote the values significant at the 90% confidence level from a two-tailed Student's *t* test

between the Arctic and mid-latitude air masses, although negative anomalies over East Asia are not significant (Figure 4a). Correspondingly, pronounced positive SLP anomalies are seen over Siberia and negative anomalies are seen over mid-latitudes (Figure 4b), resulting in dry conditions north of Siberia and Lena (approximately 60°−70°N), and wet conditions west of Baikal (Figure 4c). During the period of 1997–2016, in contrast, positive geopotential height anomalies extend further southeastward to East Asia than they did from 1980–1996, along with negative anomalies over China and west Pacific (Figure 4d). Meanwhile, positive and negative SLP anomalies are observed over central Siberia and northeastern China from 1997 to 2016, respectively (Figure 4e), along with dry and wet conditions over high and mid-latitudes, respectively (Figure 4f). Hence, decreasing sea ice-related atmospheric circulation anomalies are different between the 1997–2016 period and the 1980–1996 period.

Boreal atmospheric circulation and precipitation anomalies during these two sub-periods could generate different

surface condition patterns in their following seasons. In particular, the moisture source of the anomalous positive snow depth over West Siberia could be the result of Arctic sea ice loss (Wegmann, 2015). Figures 5 and 6 display the regressed snow depth and soil moisture anomalies in subsequent seasons onto the SIC index. During the period 1997–2014 (lack of 2015 and 2016 snow depth data), when the SIC decreases in autumn, a dipole pattern of snow depth anomalies occurs over Siberia, featured by significant positive over the south part of the Siberian region and northeastern China and negative anomalies over Siberia during wintertime (Figure 5d). This pattern of snow depth anomalies could persist until the successive spring due to the temperature lower than 0°C in cold seasons (Figure 5e,f). However, during the period 1982–1996, the anomalous pattern of snow depth moves northward and the most significant negative anomalies appear in the region of east of Ural (Figure 5a). The same pattern is also seen until following spring during cold seasons (Figure 5b,c).

In light of its features of high albedo and low conductivity, snow greatly influences the boundary-layer climate (Bednorz, 2004), related to the varying such as air temperature, precipitation and soil conditions. Soil moisture conditions may also persist through the frozen season of winter and spring. Corresponding to the autumn precipitation anomalies associated with lower SIC (Figure 4), negative soil moisture anomalies from autumn to spring are statistically significant over Siberia in both periods (Figure 6), although there are some differences between 1980–1996 and 1997–2016. Soil moisture anomalies during 1980–1996 mainly appear over west and central Siberia (Figure 6a–c); however, anomalies move eastward and appear over central Siberia during 1997–2016 (Figure 6d–f). In addition, the above-normal soil moisture

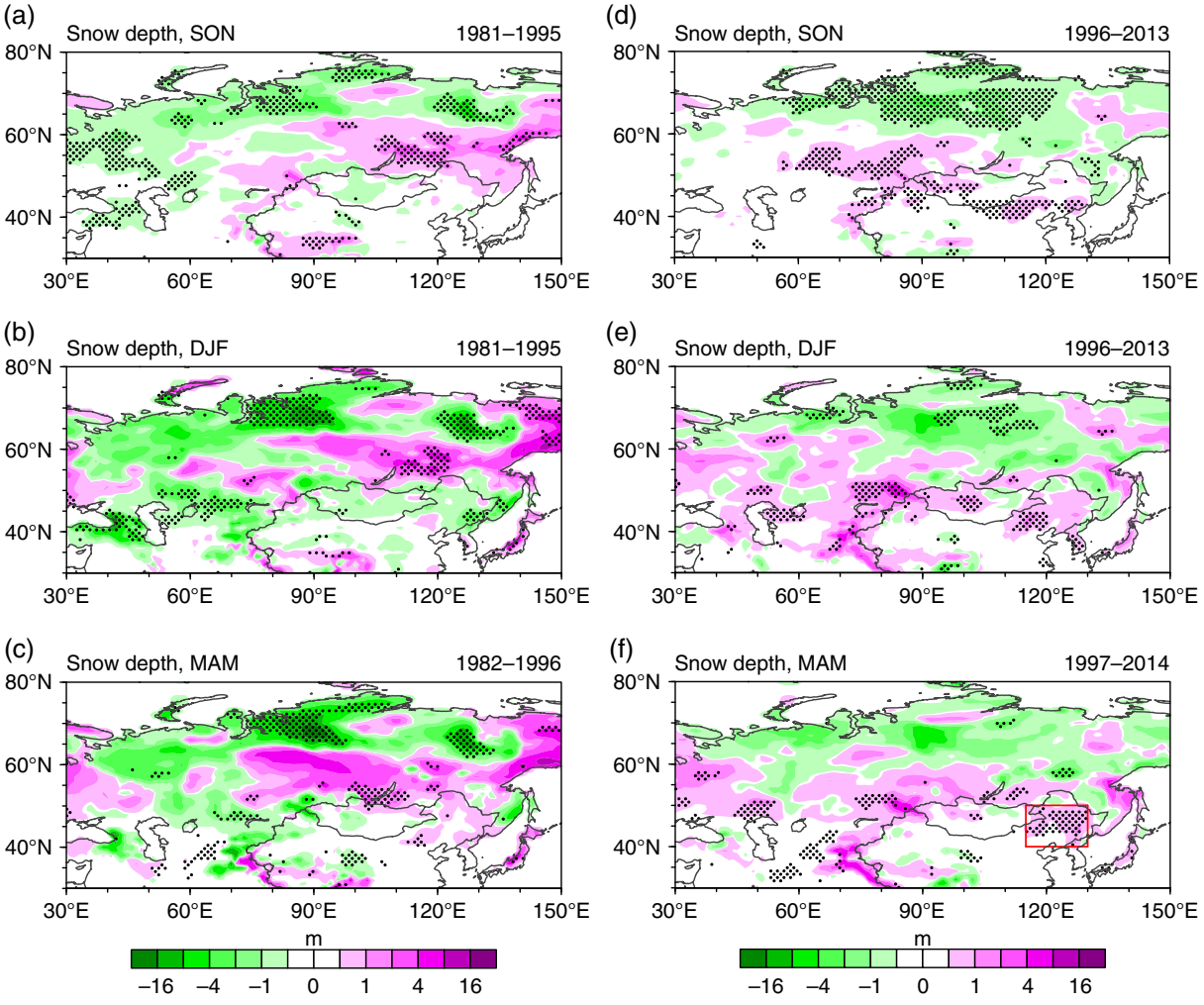

FIGURE 5 Regression maps of (a) autumn, (b) winter and (c) spring snow depth anomalies (m) with regard to autumn SIC index during 1981/1982–1995/96. The right panel (d–f) is the same as the left panel (a–c), but for 1996/1997–2013/2014. Stippled regions denote the values significant at the 90% confidence level from a two-tailed Student's *t* test. Red box in (f) indicate regions where the snow depth is averaged to obtain the SD

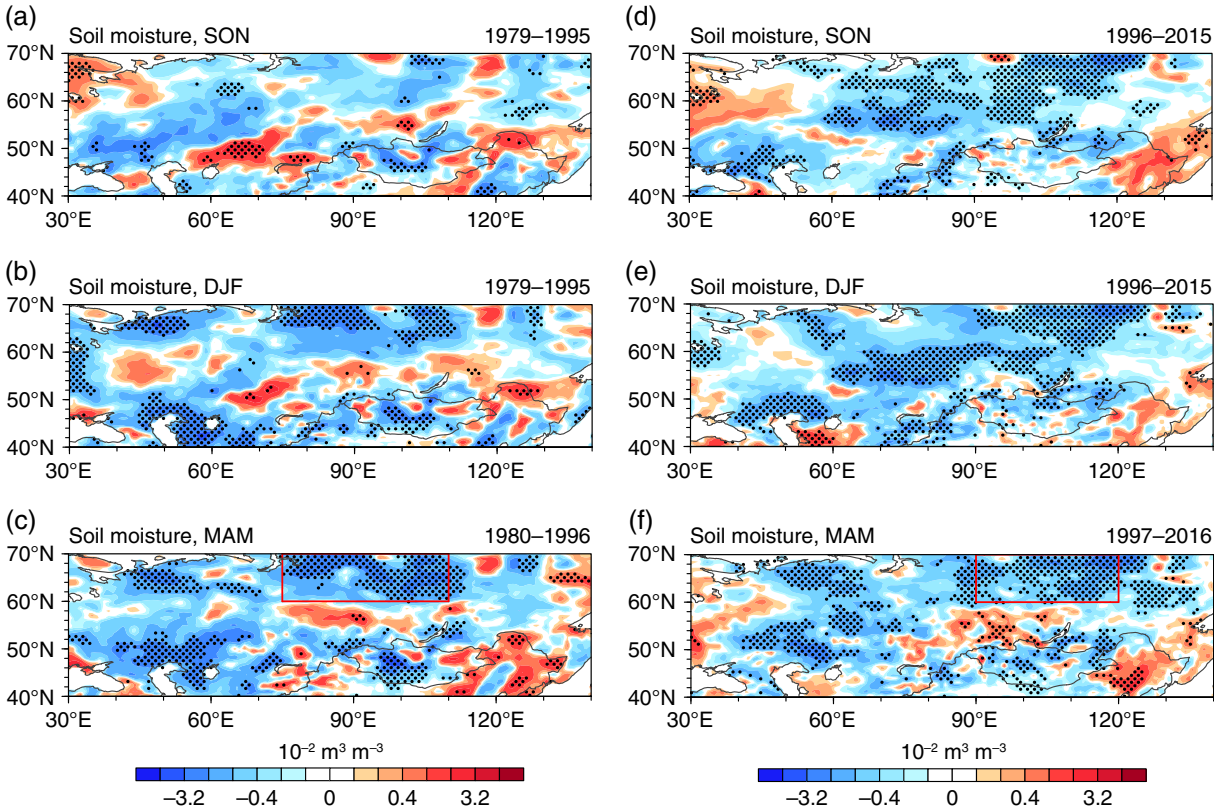

FIGURE 6 Regression maps of (a) autumn, (b) winter and (c) spring soil moisture anomalies (10^{-2} m^3 m^{-3}) with regard to autumn SIC index during 1979/1980–1995/1996. The right panel (d–f) is the same as the left panel (a–c), but for 1996/1997–2015/2016. Stippled regions denote the values significant at the 90% confidence level from a two-tailed Student's *t* test. Red boxes in (c) and (f) panel indicate regions where the soil moisture is averaged to obtain the SM2 and SM1, respectively

over northeastern China during 1997–2016 becomes significant during spring due to the thawing processes of snow (Figure 6f). In addition, the soil moisture anomalies from the CPC and MERRA-2 data support the results from the ERA-Interim data (figure not shown).

These results indicate that variations in snow depth and soil moisture are coherent and that the signal of decreasing Arctic sea ice can be retained in both snow depth and soil moisture conditions in subsequent seasons because of the large thermal inertia of snow and soil (Charney and Shukla, 1981). Snow depth, on one hand, can influence climate through albedo effect; on the other, it can impact soil moisture by initiating a delayed hydrological effect on seasonal timescales and further affecting atmospheric circulation (Cohen and Rind, 1991; Ogi *et al*., 2003; Edwards *et al*., 2007; Yang *et al*., 2016; Halder and Dirmeyer, 2017). We picked two soil moisture indices (SM) for each period based on the soil moisture anomalies over the Eurasian continent. Abnormally dry spring soil region associated with positive surface air temperature anomaly and deficient surface specific humidity tend to trigger large-scale planetary wave and remotely atmospheric circulation via soil moisture–atmosphere feedback (Douville, 2002; Van den Dool *et al*., 2003; Lau and Kim, 2012; Koster *et al*., 2014). For the period 1997–2016, SM1 is calculated as the regional mean area-weighted soil moisture anomalies over the region of 60°−70°N, 90°−120°E (represented by the red frame in Figure 6f) and is used to examine the link between spring soil processes and summer atmospheric circulation (Figures 7a and 8a,b). Drier than normal Siberian soil tends to enhance positive height anomalies at 500 hPa along with an obvious wave train structure that originates in Siberia and expands southward to Baikal and central East Asia (Figure 7a). This positive feedback, drier soil inducing anticyclonic circulation, is in good agreement with previous studies (Fischer *et al*., 2007; Seneviratne *et al*., 2010). Such a wave train may transport the soil moisture anomaly signal from high latitudes to mid-latitudes, and then produce anomalous circulations over East Asia. Meanwhile, negative and positive SLP anomalies appear over central Eurasian and south of Japan, respectively (Figure 8a). As a result, a large amount of water vapour is transmitted into Northeastern China, and less moisture is transmitted into the south of Japan due to the anomalous southerly winds, which contribute to a dipole pattern of precipitation anomalies over East Asia (Figure 8b). These

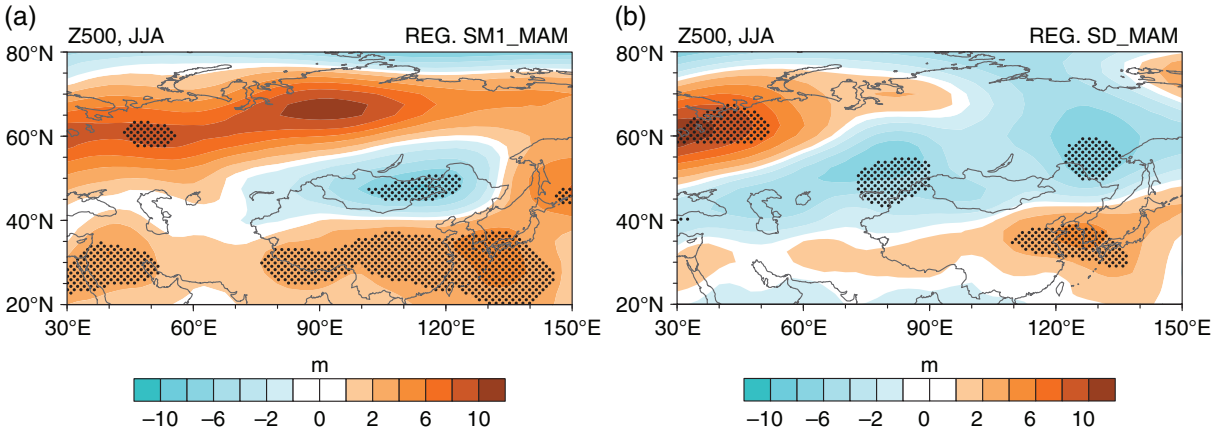

FIGURE 7 Regression of geopotential height anomalies at 500 hPa (m) with regard to (a) spring SM1 during 1997–2016 and (b) SD during 1997–2014. Stippled regions denote the values significant at the 90% confidence level from a two-tailed Student's *t* test

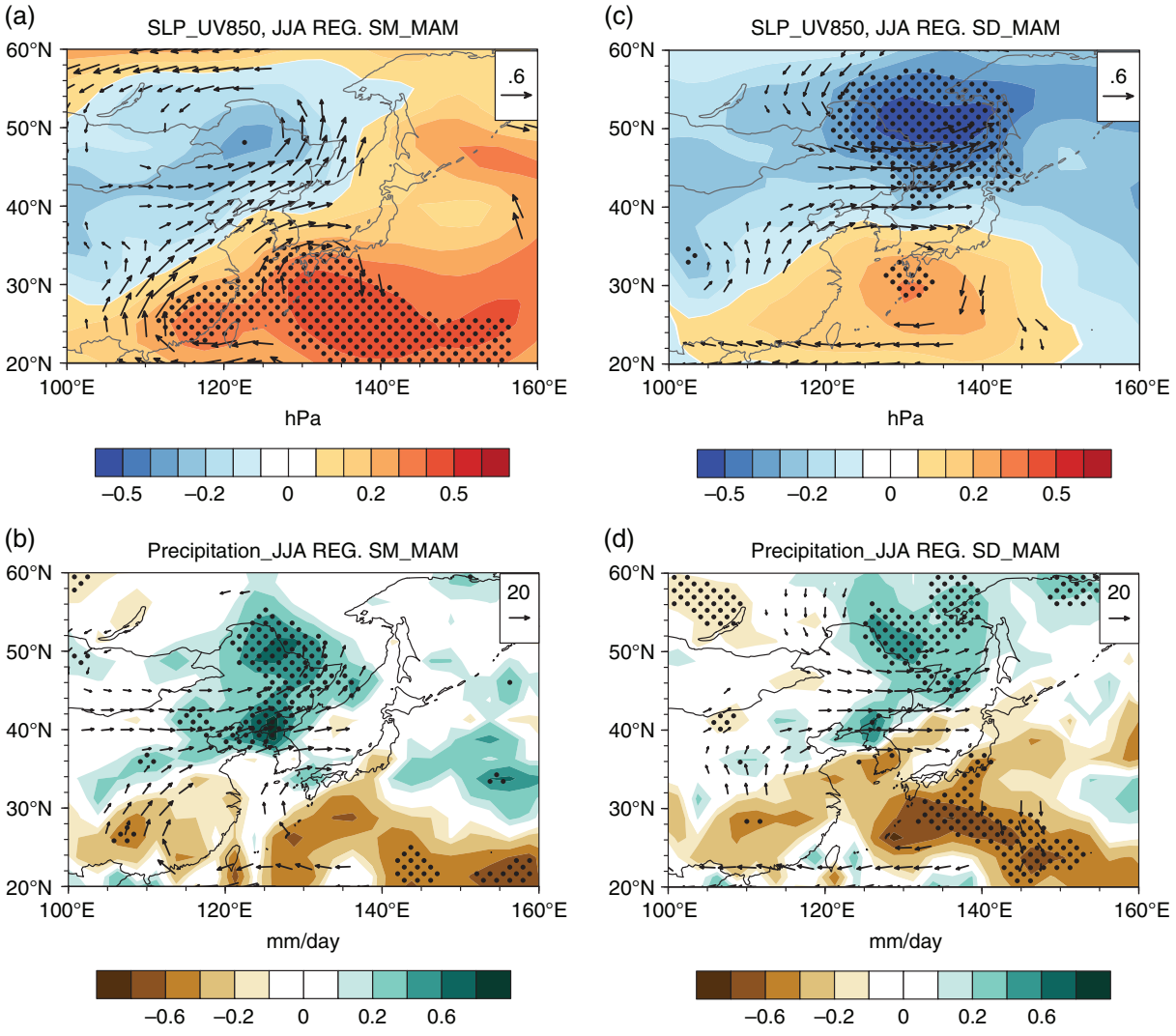

FIGURE 8 Regression of (a) SLP (shading; hPa) and winds at 850 hPa (vectors; m/s) and (b) vertically integrated water vapour transport vector (kg m^{-1} s^{-1}; from the surface to 300 hPa) and precipitation anomalies (shading; mm/day) with regard to spring SM1 during 1996/1997–2015/2016. (c–d) same as (a–b), but with regard to SD. Stippled regions denote the values significant at the 90% confidence level from a two-tailed Student's *t* test

results bear a close resemblance to those associated with autumn Arctic sea ice loss (Figure 3d).

Additionally, for the period 1980–1996, another SM (SM2) index is constructed by area-weighted averaging soil moisture anomalies over the region of 60°−70°N, 75°−110°E (represented by the red frame in Figure 6c) and is used to examine the spring soil moisture's local effect on summer circulation (Figure 9). Abnormally dry spring soil over west and central Siberia favours reduced the sea level pressure (Figure 9a) and tends to induce wet conditions locally (Figure 9b). These results are similar to those associated with autumn Arctic sea ice loss (Figure 3a). Such negative soil moisture-precipitation feedback is supported by Findell and Eltahir (1999): negative soil moisture anomalies yield higher Bowen ratios and deeper planetary boundary layers, and further trigger convection. It is worth noting that interaction between soil moisture and precipitation depends on the land features and climate (Koster *et al*., 2004; Hohenegger *et al*., 2009).

Snowpack will greatly influence large-scale atmospheric circulation via both albedo and hydrological effect (Cohen and Rind, 1991; Morinaga *et al*., 2003; Halder and Dirmeyer, 2017). Additional examinations are conducted using the positive snow depth anomalies over northern East Asia during the period 1997–2016 to examine the effect of snowpack on summer circulation. Figures 7b and 8c,d illustrate that the circulation and precipitation anomalies regressed on the snow depth index (SD), which is constructed by area-weighted averaging spring snow depth anomalies over 40°−50°N, 115°−130°E (represented by the red frame in Figure 5d). High-level geopotential height anomalies, associated with positive snow depth anomalies over northeastern China, tend to show a dipole structure over East Asia, which is characterized by negative and positive anomalous centres over the north and south, respectively (Figure 7b). This dipole pattern is also obvious in the anomalous SLP field, with positive anomalies south of Japan and negative anomalies over northeastern East Asia (Figure 8c). Consequently, positive and negative precipitation anomalies occur over Northeastern East Asia and south of Japan, respectively, resulting in a dipole pattern of East Asian precipitation anomalies (Figure 8d). These results resemble those associated with autumn Arctic sea ice loss (Figure 3d). These results show that the signal of snow depth is associated with anomalous dry and wet conditions south of Japan and in northern East Asia, paralleling the distributions shown in Figures 3d and 8b. This result indicates that the signals of Arctic sea ice decline tend to persist through the thermal inertia of both snow and soil moisture from winter to spring.

Therefore, these results clarify the distinct relationship of SIC-EASP before and after the late-1990s. During the period 1997–2016, the enhanced linkage between autumn SIC over Kara-Laptev Seas and EASP may be interpreted as follows. Associated with the decline of SIC, on the one hand, the excessive spring snow/soil moisture anomalies over northeastern China can induce anomalous summer atmospheric circulation over East Asia. On the other hand, the soil moisture anomalies over central Siberia can affect the anomalous pattern of EASP remotely. The autumn Arctic sea ice declines and precipitation anomalies over East Asia are thus linked together through both the local and remote impact. Besides, during the period 1980–1996, associated atmospheric circulation and land condition anomalies are apparent over the Siberian region, instead of East Asia, suggesting a weak relationship between sea ice and EASP.

The above results highlight the role of land surface processes in the linkage of autumn sea ice and subsequent summer precipitation anomalies over East Asia. As reported by the National Snow and Ice Data Center (NSIDC), the Arctic sea ice extent reached an extremely low value for the satellite era during September 2012. The autumn SIC in the Kara–Laptev Seas also shows extreme values during the past

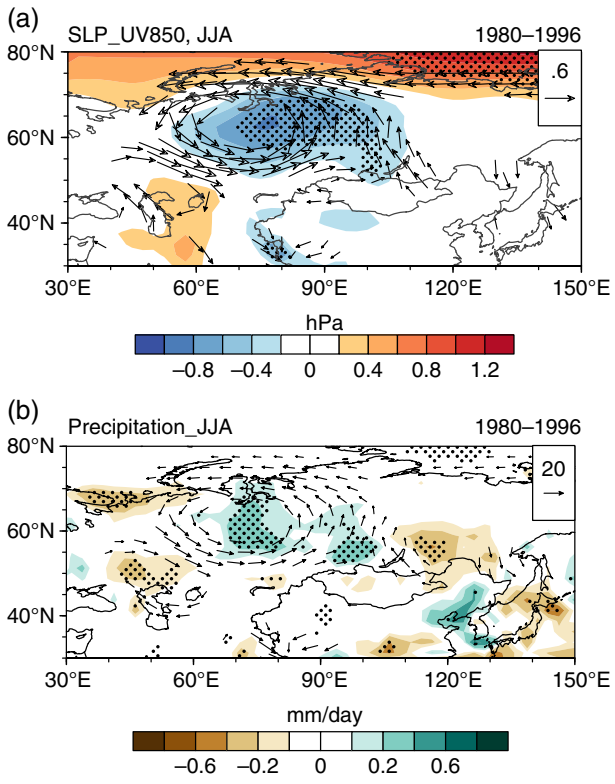

FIGURE 9 Regression of (a) SLP (shading; hPa) and winds at 850 hPa (vectors; m/s) and (b) vertically integrated water vapour transport vector (kg m^{-1} s^{-1}; from the surface to 300 hPa) and precipitation anomalies (shading; mm/day) with regard to spring SM2 during 1979/1980–1995/1996. Stippled regions denote the values significant at the 90% confidence level from a two-tailed Student's *t* test

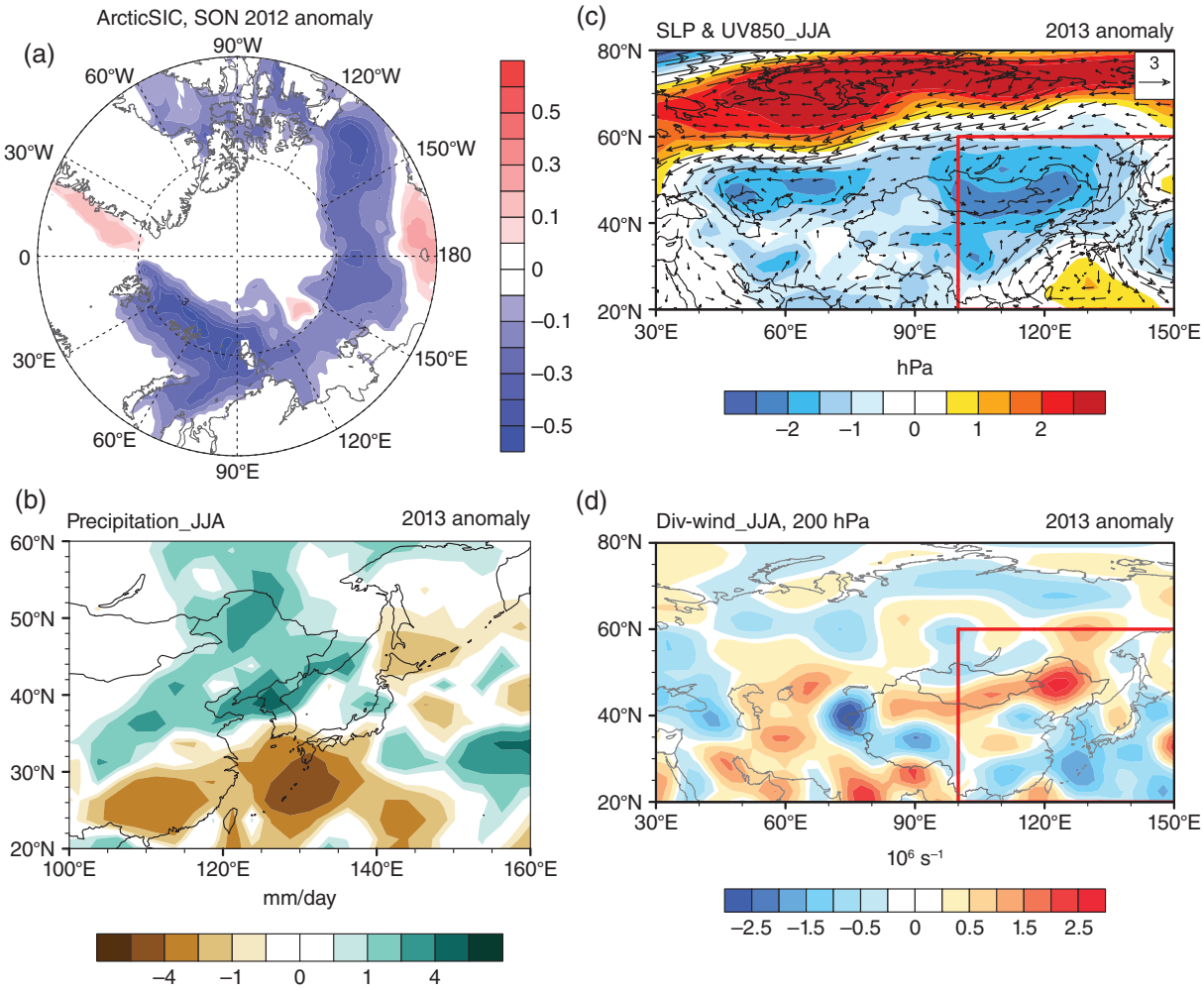

FIGURE 10 The anomalies of (a) Arctic SIC during autumn of 2012, (b) precipitation (mm/day), (c) SLP (shading; hPa) and winds at 850 hPa (vectors; m/s) and (d) divergence at 200 hPa (10^{-6} s^{-1}) during summer of 2013 (relative to the climatology of 1981–2010)

three decades (Figure 1). We use the year 2012/2013 to confirm the significant relationship that exists after the late-1990s between SIC and EASP. Figure 10 shows the spatial patterns of anomalous autumn SIC in 2012, as well as summer precipitation and relevant circulation patterns with respect to the climatology of 1981–2010. Obviously, in the autumn of 2012, there were strong negative SIC anomalies over both the Kara–Laptev Seas and the Beaufort Sea, suggesting a low amount of sea ice (Figure 10a). Correspondingly, the 2012 autumn snow depth anomaly shows negative values over central Siberia, and positive values over southern Siberia and northeastern China (Figure 11a). This anomalous pattern could persist into the subsequent seasons (Figure 11b,c). Positive (negative) snow depth anomalies generally result in more (less) soil moisture in the southern Siberia and northeastern China (Siberia; Figure 11d–f). Due to the combined effects of snow depth and soil moisture, a dipole structure of anomalous precipitation is observed over East Asia in the summer of 2013 (Figure 10b), along with an anomalous low-level cyclonic (anticyclonic) circulation and an upward (downward) motion over northeastern East Asia (south of Japan; Figure 10c,d). The scenario in 2012/2013 further confirms the linkage between SIC and EASP and highlights the important role of land surface processes (Figures 5e,f and 6e,f).

5 | SUMMARY AND DISCUSSION

In this study, we have shown interannual covariation between East Asian anomalous summer precipitation patterns and autumn Arctic sea ice loss in the Kara–Laptev Seas. During the period 1997–2016, associated with autumn Arctic sea ice loss, anomalous wet and dry conditions tend to occur over East Asia and south of Japan, respectively. In contrast, the declining sea ice exerts little influence on the EASP during 1980–1996. The possible physical mechanism for the relationship between autumn Arctic sea ice and

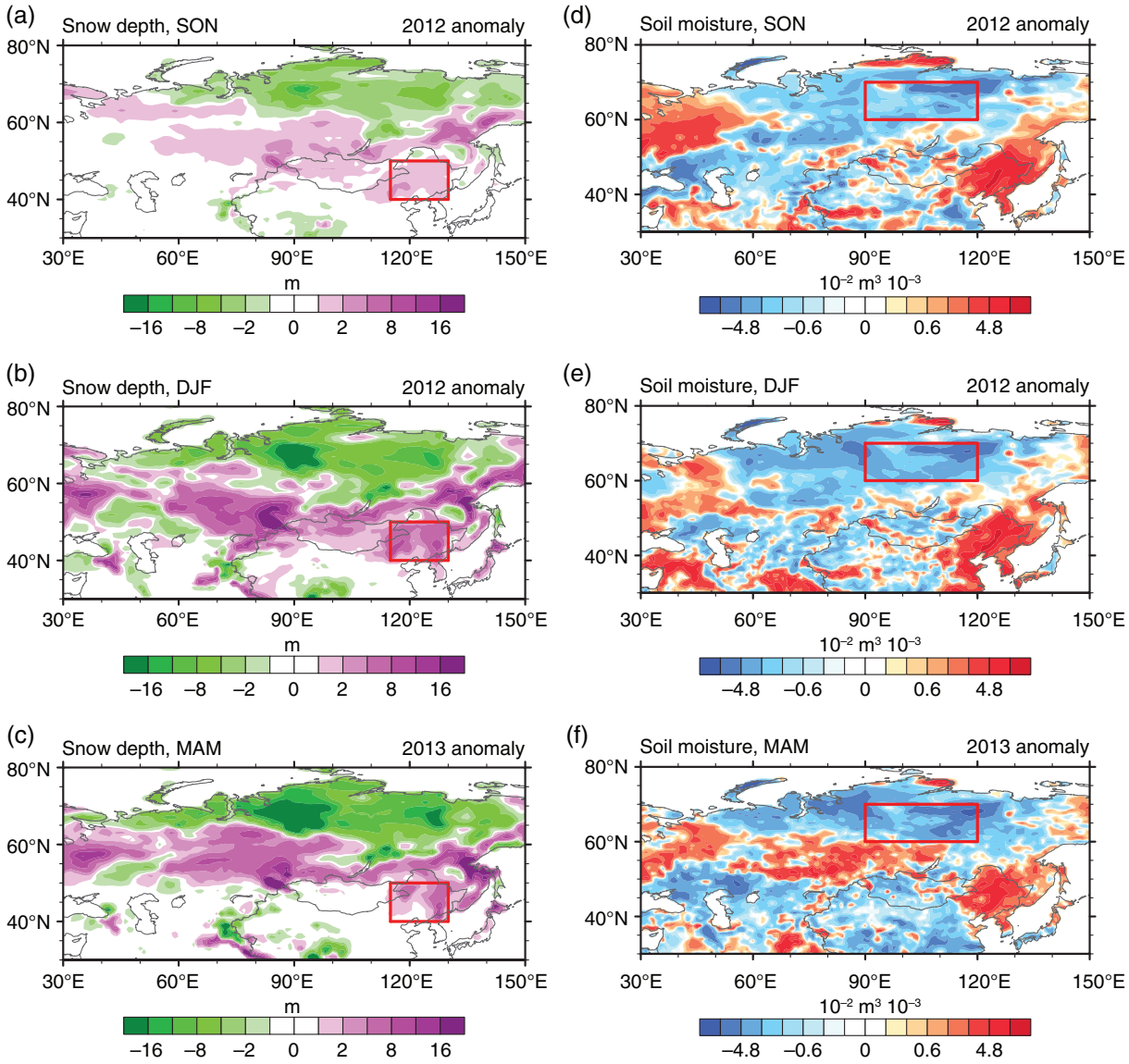

FIGURE 11 Snow depth anomalies (m) during (a) autumn and (b) winter of 2012 and (c) spring of 2013 (relative to the climatology of 1981–2010). (d–f) Same as (a–c) but for soil moisture anomalies (10^{-2} m^3 m^{-3})

summer precipitation is proposed as follows. For the period 1997–2016, Arctic sea ice loss is associated with simultaneous variations in mid-latitude climate. Anomalous positive SLP could extend southward to East Asia, accompanied by negative anomalies over northeastern China. Anomalous atmospheric circulation and moisture conditions appear to be relevant to contemporaneous land surface variations on the Eurasian continent. In addition, the anomalous pattern of snow depth and soil moisture may exhibit little change until the subsequent spring because of freezing processes. When autumn sea ice is below normal, anomalous dry soil conditions continuously appear over the central Siberian region in subsequent seasons. Abnormal soil moisture affects surface parameters (e.g., surface air temperature, specific humidity) and leads to interaction with atmosphere. In addition, negative soil moisture anomalies over central Siberia are associated with the presence of a north–south wave train structure in summer, and they generate circulation anomalies over East Asia. In addition, snowmelt itself could have impacts on atmospheric circulation by changing summer heat and moisture fluxes. The excessive snow depth anomalies over northeastern China are associated with significant anticyclonic and cyclonic circulation anomalies over East Asia and lead to anomalous positive precipitation anomalies over northeastern East Asia and negative anomalies south of Japan. Moreover, the scenario in 2012/2013 confirms this relationship and stresses the importance of land surface processes.

In addition to the observational analysis, CESM-LE simulations are employed to further examine the proposed

physical processes. We select the four lowest (highest) SIC and there is a robust relationship between SIC and EASP. We analyse each member first and then assess the differences between all members. Figure 12a illustrates the composite maps of autumn Arctic sea ice between four low and four high SIC years after the late-1990s based on 40 ensemble members of CESM-LE. A significant decline in the SIC in the Kara–Laptev Seas is observed between years of low and high SIC. Subsequently, a decline in autumn SIC favours decreased (increased) soil moisture and snow depth over central Siberia (northeastern China) from autumn until the following spring (only the spring scenario is shown in Figure 12b,c), which is consistent with the observational results (Figures 5 and 6). Following the decline in autumn SIC, the anomalous summer precipitation pattern can be partly observed over East Asia (Figure 12d). Accordingly, a decrease in soil moisture is seen from low to high SM1 (Figure 12e). Therefore, the linkage between the autumn

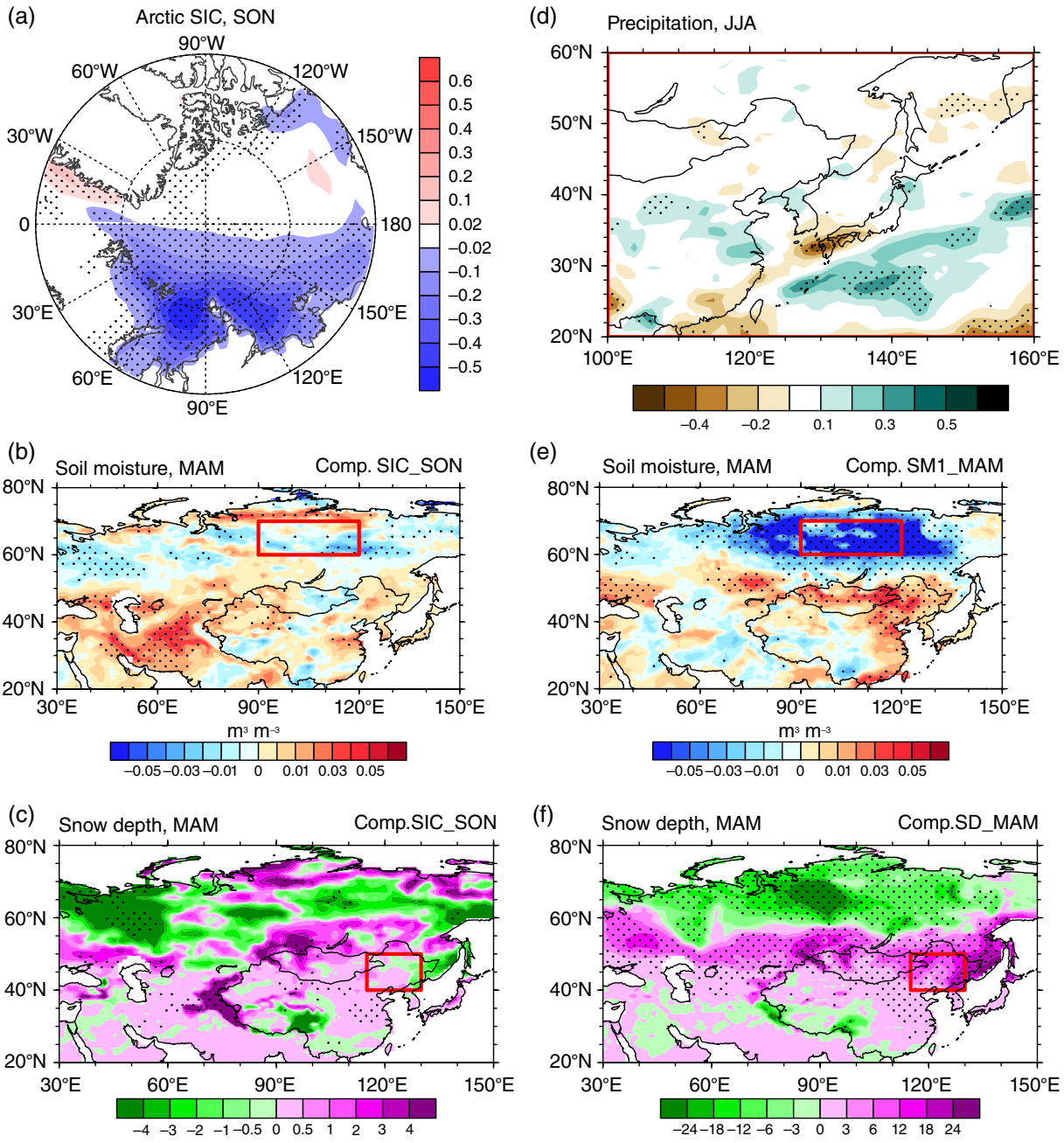

FIGURE 12 Composite maps of (a) Arctic SIC in autumn, (b) soil moisture ($m^3\ m^{-3}$) in spring, (c) snow depth (m) in spring and (d) precipitation (mm/day) in summer between four low and four high SIC years from 1996/1997–2016/2017. Composite maps of (e) spring soil moisture between four low and four high years of SM1 and (f) spring snow depth between four high and low years of SD during 1997–2017. Stippled regions denote the values significant at the 90% confidence level from a two-tailed Student's *t* test. The results are calculated from 40 ensembles of CESM-LE

SIC loss in the Kara–Laptev Seas and summer atmospheric circulation also exists in the model simulations. In addition, the association with physical processes, such as soil moisture and snow depth, is also supported by model results. The state-of-the-art models have a limited capability (such as internal variability and model uncertainties) to simulate the East Asian summer rainfall, so it is understandable that the summer precipitation anomalies are not well captured by CESM-LE. The present analysis demonstrates that the autumn–spring snow depth and autumn–spring soil moisture might be climatic factors that retain the signal of autumn sea ice anomalies and then influence the summer atmospheric circulation over Eurasia.

Our present study highlights that the linkage of autumn sea ice and subsequent summer precipitation anomalies over East Asia is unstable, and this linkage becomes significant after the late 1990s. These results have important implications for extending the seasonal prediction validity of EASP. The long-term memory of land surface processes including the soil moisture and snow depth over Eurasia are suggested to be key factors connecting the SIC and EASP. However, several problems remain unresolved. For example, the detailed land–air progresses remain much less acknowledged compared to the air–sea interaction, and more in-depth analysis in terms of land–air interaction need to be performed. Above analysis cannot separate the relative contributions of soil moisture and snow depth to summertime atmospheric circulation anomalies, and this issue demands further exploration via simulations. Land surface processes can bridge the autumn SIC and EASP via slow variations in the cold season, but other processes, such as stratosphere–troposphere coupling and air–sea interaction, may also play a role in the linkage between SIC and EASP. What are their relative contributions to the linkage between SIC and EASP? In addition, an extension of this study would be to examine the linkage between Arctic sea ice loss and summer climate variation in other regions of the Northern Hemisphere.

ACKNOWLEDGEMENTS

This research was supported by the National Key Research and Development Program of China (Grant No. 2016YFA0600701), National Natural Science Foundation of China (41611130043, 41675083 and 41605064) and the CAS–PKU Joint Research Program.

ORCID

Yang Liu https://orcid.org/0000-0002-8769-2323
Jianqi Sun https://orcid.org/0000-0002-3879-6986
Alla Yurova https://orcid.org/0000-0001-6199-414X

REFERENCES

Adler, R.F., Huffman, G.J., Chang, A., Ferraro, R., Xie, P.P., Janowiak, J., Rudolf, B., Schneider, U., Curtis, S., Bolvin, D., Gruber, A., Susskind, J., Arkin, P. and Nelkin, E. (2003) The version-2 global precipitation climatology project (GPCP) monthly precipitation analysis (1979–present). *Journal of Hydrometeorology*, 4(6), 1147–1167.

Bader, J., Mesquita, M.D., Hodges, K.I., Keenlyside, N., Østerhus, S. and Miles, M. (2011) A review on Northern Hemisphere Sea-ice, storminess and the North Atlantic oscillation: observations and projected changes. *Atmospheric Research*, 101(4), 809–834. https://doi.org/10.1016/j.atmosres.2011.04.007.

Bednorz, E. (2004) Snow cover in eastern Europe in relation to temperature, precipitation and circulation. *International Journal of Climatology*, 24(5), 591–601. https://doi.org/10.1002/joc.1014.

Bosilovich, M.G. S. Akella, L. Coy, R. Cullather, C. Draper, R. Gelaro, R. Kovach, Q. Liu, A. Molod, P. Norris, K. Wargan, W. Chao, R. Reichle, L. Takacs, Y. Vikhliaev, S. Bloom, A. Collow, S. Firth, G. Labow, G. Partyka, S. Pawson, O. Reale, S. D. Schubert, and M. Suarez. (2015). *MERRA-2: Initial evaluation of the climate. NASA Technical Report Series on Global Modeling and Data Assimilation*. NASA/TM-2015-104606, 43, 145. Available at: https://gmao.gsfc.nasa.gov/pubs/tm/docs/Bosilovich803.pdf.

Bretherton, C.S., Smith, C. and Wallace, J.M. (1992) An intercomparison of methods for finding coupled patterns in climate data. *Journal of Climate*, 5(6), 541–560.

Budikova, D. (2009) Role of Arctic Sea ice in global atmospheric circulation: a review. *Global and Planetary Change*, 68(3), 149–163. https://doi.org/10.1016/j.gloplacha.2009.04.001.

Charney, J. and Shukla, J. (1981) Predictability of monsoons. In: Lighthill, J. and Pearce, R. (Eds.) *Monsoon Dynamics*. Cambridge: Cambridge University Press, pp. 99–110.

Chiang, J.C.H., Swenson, L.M. and Kong, W. (2017) Role of seasonal transitions and the westerlies in the interannual variability of the East Asian summer monsoon precipitation. *Geophysical Research Letters*, 44(8), 3788–3795. https://doi.org/10.1002/2017GL072739.

Cohen, J. and Rind, D. (1991) The effect of snow cover on the climate. *Journal of Climate*, 4(7), 689–706.

Cohen, J., Furtado, J.C., Jones, J., Barlow, M., Whittleston, D. and Entekhabi, D. (2014) Linking Siberian snow cover to precursors of stratospheric variability. *Journal of Climate*, 27(14), 5422–5432. https://doi.org/10.1175/JCLI-D-13-00779.1.

Curry, J.A., Schramm, J.L. and Ebert, E.E. (1995) Sea ice-albedo climate feedback mechanism. *Journal of Climate*, 8(2), 240–247. https://doi.org/10.1175/1520-0442(1995)008<0240:SIACFM>2.0.CO;2.

Dee, D., Uppala, S., Simmons, A., Berrisford, P., Poli, P., Kobayashi, S., Andrae, U., Balmaseda, M.A., Balsamo, G., Bauer, P., Bechtold, P., Beljaars, A.C.M., van de Berg, L., Bidlot, J., Bormann, N., Delsol, C., Dragani, R., Fuentes, M., Geer, A.J., Haimberger, L., Healy, S.B., Hersbach, H., Hólm, E.V., Isaksen, L., Kållberg, P., Köhler, M., Matricardi, M., McNally, A. P., Monge-Sanz, B.M., Morcrette, J.-J., Park, B.-K., Peubey, C., de Rosnay, P., Tavolato, C., Thépaut, J.-N. and Vitart, F. (2011) The ERA-interim reanalysis: configuration and performance of the data assimilation system. *Quarterly Journal of the Royal Meteorological Society*, 137(656), 553–597. https://doi.org/10.1002/qj.828.

Deser, C., Tomas, R., Alexander, M. and Lawrence, D. (2010) The seasonal atmospheric response to projected Arctic Sea ice loss in the late twenty-first century. *Journal of Climate*, 23(2), 333–351. https://doi.org/10.1175/2009JCLI3053.1.

Ding, Q. and Wang, B. (2005) Circumglobal teleconnection in the northern hemisphere summer. *Journal of Climate*, 18(17), 3483–3505. https://doi.org/10.1175/JCLI3473.1.

Douville, H. (2002) Influence of soil moisture on the Asian and African monsoons. Part II: interannual variability. *Journal of Climate*, 15 (7), 701–720. https://doi.org/10.1175/1520-0442(2002)015,0701: IOSMOT.2.0.CO;2.

Edwards, A.C., Scalenghe, R. and Freppaz, M. (2007) Changes in the seasonal snow cover of alpine regions and its effect on soil processes: a review. *Quaternary International*, 162, 172–181. https://doi.org/10.1016/j.quaint.2006.10.027.

Entin, J.K., Robock, A., Vinnikov, K.Y., Hollinger, S.E., Liu, S. and Namkhai, A. (2000) Temporal and spatial scales of observed soil moisture variations in the extratropics. *Journal of Geophysical Research-Atmospheres*, 105(D9), 11865–11877. https://doi.org/10.1029/2000JD900051.

Fan, Y. and van den Dool, H. (2004) Climate prediction center global monthly soil moisture data set at 0.5 resolution for 1948 to present. *Journal of Geophysical Research-Atmospheres*, 109(D10), D10102. https://doi.org/10.1029/2003JD004345.

Findell, K.L. and Eltahir, E.A. (1999) Analysis of the pathways relating soil moisture and subsequent rainfall in Illinois. *Journal of Geophysical Research-Atmospheres*, 104(D24), 31565–31574. https://doi.org/10.1175/1525-7541(2003)004<0552:ACOSML>2.0.CO;2.

Fischer, E.M., Seneviratne, S.I., Vidale, P.L., Lüthi, D. and Schär, C. (2007) Soil moisture–atmosphere interactions during the 2003 European summer heat wave. *Journal of Climate*, 20(20), 5081–5099. https://doi.org/10.1175/JCLI4288.1.

Francis, J.A. and Vavrus, S.J. (2012) Evidence linking Arctic amplification to extreme weather in mid-latitudes. *Geophysical Research Letters*, 39(6), L06801. https://doi.org/10.1029/2012GL051000.

Fu, Y. and Lu, R. (2017) Improvements in simulating the relationship between ENSO and East Asian summer rainfall in the CMIP5 models. *Journal of Climate*, 30(12), 4513–4525. https://doi.org/10.1175/JCLI-D-16-0606.1.

Gao, Y., Sun, J., Li, F., He, S., Sandven, S., Yan, Q., Zhang, Z., Lohmann, K., Keenlyside, N., Furevik, T. and Suo, L. (2015) Arctic Sea ice and Eurasian climate: a review. *Advances in Atmospheric Sciences*, 32(1), 92–114. https://doi.org/10.1007/s00376-014-0009-6.

Guo, D., Gao, Y., Bethke, I., Gong, D., Johannessen, O.M. and Wang, H. (2014) Mechanism on how the spring Arctic Sea ice impacts the East Asian summer monsoon. *Theoretical and Applied Climatology*, 115(1–2), 107–119. https://doi.org/10.1007/s00704-013-0872-6.

Halder, S. and Dirmeyer, P.A. (2017) Relation of Eurasian snow cover and Indian summer monsoon rainfall: importance of the delayed hydrological effect. *Journal of Climate*, 30(4), 1273–1289. https://doi.org/10.1175/JCLI-D-16-0033.1.

Hohenegger, C., Brockhaus, P., Bretherton, C.S. and Schär, C. (2009) The soil moisture–precipitation feedback in simulations with explicit and parameterized convection. *Journal of Climate*, 22(19), 5003–5020. https://doi.org/10.1175/2009JCLI2604.1.

Hsu, H.H. and Lin, S.M. (2007) Asymmetry of the tripole rainfall pattern during the East Asian summer. *Journal of Climate*, 20(17), 4443–4458. https://doi.org/10.1175/JCLI4246.1.

Hsu, H.H. and Liu, X. (2003) Relationship between the Tibetan plateau heating and East Asian summer monsoon rainfall. *Geophysical Research Letters*, 30(20), 2066. https://doi.org/10.1029/2003GL017909.

Hurrell, J.W., Holland, M.M., Gent, P.R., Ghan, S., Kay, J.E., Kushner, P.J., Ghan, S., Kay, J.E., Kushner, P.J., Lamarque, J.-F., Large, W.G., Lawrence, D., Lindsay, K., Lipscomb, W.H., Long, M.C., Mahowald, N., Marsh, D.R., Neale, R.B., Rasch, P., Vavrus, S., Vertenstein, M., Bader, D., Collins, W.D., Hack, J.J., Kiehl, J., Marshall, S. and Lindsay, K. (2013) The community earth system model: a framework for collaborative research. *Bulletin of the American Meteorological Society*, 94(9), 1339–1360. https://doi.org/10.1175/BAMS-D-12-00121.1.

Kanamitsu, M., Ebisuzaki, W., Woollen, J., Yang, S.K., Hnilo, J.J., Fiorino, M. and Potter, G.L. (2002) NCEP–DOE AMIP-II reanalysis (R-2). *Bulletin of the American Meteorological Society*, 83(11), 1631–1644. https://doi.org/10.1175/BAMS-83-11-1631.

Kay, J.E., Deser, C., Phillips, A., Mai, A., Hannay, C., Strand, G., Arblaster, J.M., Bates, S.C., Danabasoglu, G., Edwards, J., Holland, M., Kushner, P., Lamarque, J.F., Lawrence, D., Lindsay, K., Middleton, A., Munoz, E., Neale, R., Oleson, K., Polvani, L. and Vertenstein, M. (2015) The community earth system model (CESM) large ensemble project: a community resource for studying climate change in the presence of internal climate variability. *Bulletin of the American Meteorological Society*, 96(8), 1333–1349. https://doi.org/10.1175/BAMS-D-13-00255.1.

Kim, B.M., Son, S.W., Min, S.K., Jeong, J.H., Kim, S.J., Zhang, X., Shim, T. and Yoon, J.H. (2014) Weakening of the stratospheric polar vortex by Arctic Sea-ice loss. *Nature Communications*, 5, 4646. https://doi.org/10.1038/ncomms5646.

Kosaka, Y. and Nakamura, H. (2006) Structure and dynamics of the summertime Pacific–Japan teleconnection pattern. *Quarterly Journal of the Royal Meteorological Society*, 132(619), 2009–2030. https://doi.org/10.1256/qj.05.204.

Koster, R.D., Dirmeyer, P.A., Guo, Z., Bonan, G., Chan, E., Cox, P., Gordon, C.T., Kanae, S., Kowalczyk, E., Lawrence, D., Liu, P., Lu, C.-H., Malyshev, S., McAvaney, B., Mitchell, K., Mocko, D., Oki, T., Oleson, K., Pitman, A., Sud, Y.C., Taylor, C.M., Verseghy, D., Vasic, R., Xue, Y. and Yamada, T. (2004) Regions of strong coupling between soil moisture and precipitation. *Science*, 305(5687), 1138–1140. https://doi.org/10.1126/science.1100217.

Koster, R.D., Chang, Y. and Schubert, S.D. (2014) A mechanism for land–atmosphere feedback involving planetary wave structures. *Journal of Climate*, 27(24), 9290–9301. https://doi.org/10.1175/JCLI-D-14-00315.1.

Koster, R.D., Chang, Y., Wang, H. and Schubert, S.D. (2016) Impacts of local soil moisture anomalies on the atmospheric circulation and on remote surface meteorological fields during boreal summer: a comprehensive analysis over North America. *Journal of Climate*, 29(20), 7345–7364. https://doi.org/10.1175/JCLI-D-16-0192.1.

Lau, W.K. and Kim, K.M. (2012) The 2010 Pakistan flood and Russian heat wave, Teleconnection of hydrometeorological extremes. *Journal of Hydrometeorology*, 13(1), 392–403. https://doi.org/10.1175/JHM-D-11-016.1.

Li, F. and Wang, H. (2012) Autumn Sea ice cover, winter northern hemisphere annular mode, and winter precipitation in Eurasia.

Journal of Climate, 26(11), 3968–3981. https://doi.org/10.1175/JCLI-D-12-00380.1.

Liu, J., Curry, J.A., Wang, H., Song, M. and Horton, R.M. (2012) Impact of declining Arctic Sea ice on winter snowfall. *Proceedings of the National Academy of Sciences of the United States of America*, 109 (11), 4074–4079. https://doi.org/10.1073/pnas.1114910109.

McBean, G., Alekseev, G., Chen, D., Foerland, E., Fyfe, J., Groisman, P.Y., King, R., Melling, H., Vose, R. and Whitfield, P. H. (2005) Chapter 2: Arctic climate: past and present. In: *Arctic climate impact assessment*. Cambridge, MA: Cambridge University Press.

Mori, M., Watanabe, M., Shiogama, H., Inoue, J. and Kimoto, M. (2014) Robust Arctic Sea-ice influence on the frequent Eurasian cold winters in past decades. *Nature Geoscience*, 7(12), 869–873. https://doi.org/10.1038/ngeo2277.

Morinaga, Y., Tian, S.F. and Shinoda, M. (2003) Winter snow anomaly and atmospheric circulation in Mongolia. *International Journal of Climatology*, 23(13), 1627–1636. https://doi.org/10.1002/joc.961.

Nitta, T. (1987) Convective activities in the tropical western Pacific and their impact on the northern hemisphere summer circulation. *Journal of the Meteorological Society of Japan. Series II*, 65(3), 373–390. https://doi.org/10.2151/jmsj1965.65.3_373.

Ogi, M., Tachibana, Y. and Yamazaki, K. (2003) Impact of the wintertime North Atlantic oscillation (NAO) on the summertime atmospheric circulation. *Geophysical Research Letters*, 30(13), 1704. https://doi.org/10.1029/2003GL017280.

Peings, Y., Brun, E., Mauvais, V. and Douville, H. (2013) How stationary is the relationship between Siberian snow and Arctic oscillation over the 20th century? *Geophysical Research Letters*, 40(1), 183–188. https://doi.org/10.1029/2012GL054083.

Rayner, N., Parker, D.E., Horton, E., Folland, C., Alexander, L., Rowell, D., Kent, E.C. and Kaplan, A. (2003) Global analyses of sea surface temperature, sea ice, and night marine air temperature since the late nineteenth century. *Journal of Geophysical Research-Atmospheres*, 108(D14), 4407. https://doi.org/10.1029/2002JD002670.

Screen, J.A. (2013) Influence of Arctic Sea ice on European summer precipitation. *Environmental Research Letters*, 8(4), 044015. https://doi.org/10.1088/1748-9326/8/4/044015.

Screen, J.A. and Simmonds, I. (2010) Increasing fall-winter energy loss from the Arctic Ocean and its role in Arctic temperature amplification. *Geophysical Research Letters*, 37(16), 127–137. https://doi.org/10.1029/2010GRL044136.

Seneviratne, S.I., Corti, T., Davin, E.L., Hirschi, M., Jaeger, E.B., Lehner, I., Orlowsky, B. and Teuling, A.J. (2010) Investigating soil moisture–climate interactions in a changing climate: a review. *Earth-Science Reviews*, 99(3–4), 125–161. https://doi.org/10.1016/j.earscirev.2010.02.004.

Titchner, H.A. and Rayner, N.A. (2014) The met Office Hadley Centre Sea ice and sea surface temperature data set, version 2: 1. Sea ice concentrations. *Journal of Geophysical Research-Atmospheres*, 119 (6), 2864–2889. https://doi.org/10.1002/2013JD020316.

Van den Dool, H., Huang, J. and Fan, Y. (2003) Performance and analysis of the constructed analogue method applied to US soil moisture over 1981–2001. *Journal of Geophysical Research-Atmospheres*, 108(D16), 8617. https://doi.org/10.1029/2002JD003114.

Vihma, T. (2014) Effects of Arctic Sea ice decline on weather and climate: a review. *Surveys in Geophysics*, 35(5), 1175–1214. https://doi.org/10.1007/s10712-014-9284-0.

Wang, H. and He, S. (2015) The North China/Northeastern Asia severe summer drought in 2014. *Journal of Climate*, 28(17), 6667–6681. https://doi.org/10.1175/JCLI-D-15-0202.1.

Wegmann, M. (2015) Arctic moisture source for Eurasian snow cover variations in autumn. *Environmental Research Letters*, 10(5), 054015. https://doi.org/10.1088/1748-9326/10/5/054015.

Wegmann, M., Orsolini, Y., Dutra, E., Bulygina, O., Sterin, A. and Brönnimann, S. (2017) Eurasian snow depth in long-term climate reanalyses. *The Cryosphere*, 11(2), 923–935. http://doi.org/10.5194/tc-11-923-2017.

Weng, H., Lau, K.M. and Xue, Y. (1999) Multi-scale summer rainfall variability over China and its long-term link to global sea surface temperature variability. *Journal of the Meteorological Society of Japan. Series II*, 77(4), 845–857. https://doi.org/10.2151/jmsj1965.77.4_845.

Wu, B., Zhang, R., D'Arrigo, R. and Su, J. (2013) On the relationship between winter sea ice and summer atmospheric circulation over Eurasia. *Journal of Climate*, 26(15), 5523–5536. https://doi.org/10.1175/JCLI-D-12-00524.1.

Xie, S.P., Hu, K., Hafner, J., Tokinaga, H., Du, Y., Huang, G. and Sampe, T. (2009) Indian Ocean capacitor effect on indo–western Pacific climate during the summer following El Niño. *Journal of Climate*, 22(3), 730–747. https://doi.org/10.1175/2008JCLI2544.1.

Yang, K., Wang, C. and Bao, H. (2016) Contribution of soil moisture variability to summer precipitation in the northern hemisphere. *Journal of Geophysical Research-Atmospheres*, 121(20), 12,108–12,124. https://doi.org/10.1002/2016JD025644.

Yim, S.Y., Wang, B. and Kwon, M. (2014) Interdecadal change of the controlling mechanisms for east Asian early summer rainfall variation around the mid-1990s. *Climate Dynamics*, 42(5–6), 1325–1333. https://doi.org/10.1007/s00382-013-1760-6.

Zhao, P., Zhang, X., Zhou, X., Ikeda, M. and Yin, Y. (2004) The sea ice extent anomaly in the North Pacific and its impact on the east Asian summer monsoon rainfall. *Journal of Climate*, 17(17), 3434–3447. https://doi.org/10.1175/1520-0442(2004)017<3434:TSIEAI>2.0.CO;2.

Zuo, J., Ren, H.L., Wu, B. and Li, W. (2016) Predictability of winter temperature in China from previous autumn Arctic Sea ice. *Climate Dynamics*, 47(7–8), 2331–2343. https://doi.org/10.1007/s00382-015-2966-6.

How to cite this article: Liu Y, Zhu Y, Wang H, *et al.* Role of autumn Arctic Sea ice in the subsequent summer precipitation variability over East Asia. *Int J Climatol*. 2020;40:706–722. https://doi.org/10.1002/joc.6232